HHS Public Access

Author manuscript

Anat Rec (Hoboken). Author manuscript; available in PMC 2015 November 01.

Computational Fluid Dynamics (CFD) as surgical planning tool: a pilot study on middle turbinate resection

Kai Zhao, PhD[1,2], **Prashant Malhotra, MD**[2], **David Rosen, MD**[2], **Pamela Dalton, PhD**[1], and **Edmund A Pribitkin, MD**[2]

[1]Monell Chemical Senses Center, 3500 Market ST., Philadelphia, PA 19104

[2]Department of Otolaryngology, Thomas Jefferson University, 925 Chestnut Street, Philadelphia, PA 19107

Abstract

Controversies exist regarding the resection or preservation of the middle turbinate (MT) during functional endoscopic sinus surgery (FESS). Any MT resection will perturb nasal airflow and may affect the mucociliary dynamics of the osteomeatal complex. Neither rhinometry nor computed tomography (CT) can adequately quantify nasal airflow pattern changes following surgery. This study explores the feasibility of assessing changes in nasal airflow dynamics following partial MT resection using computational fluid dynamics (CFD) techniques. We retrospectively converted the pre- and post-operative CT scans of a patient who underwent isolated partial MT concha bullosa resection into anatomically accurate three-dimensional numerical nasal models. Pre- and post-surgery nasal airflow simulations showed that the partial MT resection resulted in a shift of regional airflow towards the area of MT removal with a resultant decreased airflow velocity, decreased wall shear stress and increased local air pressure. However, the resection did not strongly affect the overall nasal airflow patterns, flow distributions in other areas of the nose, or the odorant uptake rate to the olfactory cleft mucosa. Morever, CFD predicted the patient's failure to perceive an improvement in his unilateral nasal obstruction following surgery. Accordingly, CFD techniques can be used to predict changes in nasal airflow dynamics following partial MT resection. However, the functional implications of this analysis await further clinical studies. Nevertheless, such techniques may potentially provide a quantitative evaluation of surgical effectiveness and may prove useful in preoperatively modeling the effects of surgical interventions.

Keywords

Corresponding Author: Kai Zhao, Monell Chemical Senses Center, 3500 Market St., Philadelphia, PA 19104, 267-519-4935 (office & fax), kzhao@monell.org, Zhaok@alumni.upenn.edu.

Introduction

Chronic rhinosinusitis (CRS) is one of the most common medical conditions in the US, affecting an estimated 13% of adults (29.3 million people) and responsible for $5.8 billion in healthcare costs annually (National Health Interview Survey 2009, CDC). The disease may stem from diverse and complex clinical situations, including mucosa congestion, infection, inflammation, allergic response, nasal structural deformity, or prior surgical interventions. Functional endoscopic sinus surgery (FESS) is the primary treatment of CRS that is refractory to medical management. Although the post-surgery short-term success rates are reasonably high, ranging from ∼60-90%, long term relief of the symptoms can be as low as ∼30% (Stewart, Smith, Weaver, Witsell, Yueh, Hannley, and Johnson, 2004;Ho, Yuen, Tang, Wei, and Lam, 2004).

The ability to accurately predict changes to nasal airflow distribution due to surgery and the functional impact of these changes would likely improve surgical planning. Neither rhinometry nor computed tomography (CT) can adequately quantify nasal airflow pattern changes following surgery. Although physical models cast from noses of human cadavers or from CT images have been used in the past to study nasal flow (Proetz, 1951;swift and Proctor, 1977;Girardin, Bilgen, and Arbour, 1983;Hornung, Leopold, Youngentob, Sheehe, Gagne, Thomas, and Mozell, 1987;Hahn, Scherer, and Mozell, 1993), this approach is labor intensive and slow, thus precluding its use as clinical tool. Modern computational fluid dynamics (CFD) modeling techniques enable detailed prediction of airflow and odorant delivery patterns throughout the nasal cavity based on three-dimensional models derived from CT data (Keyhani, Scherer, and Mozell, 1995;Keyhani, Scherer, and Mozell, 1997;Subramaniam, Richardson, Morgan, and Kimbell, 1999;Martonen, Quan, Zhang, and Musante, 2002). Zhao *et al.* (Zhao, Scherer, Hajiloo, and Dalton, 2004;Zhao, Pribitkin, Cowart, Rosen, Scherer, and Dalton, 2006) first refined the technique so that a numerical model based on an individual patient's CT data can be generated in several days rather than months, enabling the potential clinical application to predict the sinus surgery outcome. Since then, CFD has been used successfully to determine nasal resistance and local airflow effects of inferior turbinate reduction (Wexler, Segal, and Kimbell, 2005), septal perforation (Grant, Bailie, Watterson, Cole, Gallagher, and Hanna, 2004), radical sinus surgery (Lindemann, Brambs, Keck, Wiesmiller, Rettinger, and Pless, 2005), and septal deviation, septoplasty (Ozlugedik, Nakiboglu, Sert, Elhan, Tonuk, Akyar, and Tekdemir, 2008;Garcia, Rhee, Senior, and Kimbell, 2010), either based on modifications to standard normal nasal models or based on real clinical cases.

Here, we further focused the CFD technique on a controversy that has been ongoing ever since the origination of endoscopic sinus surgery: middle turbinate resection versus preservation. As outlined by Wolf *et al.* (Wolf and Biedlingmaier, 2001), arguments for and against MT resection have been made on the basis of surgical convenience, risk of complications, postoperative care, physiologic principles and personal belief. Surgeons who favor MT resection cite improved visualization and ease of surgical antrostomy, the removal of osteitic material, decreased synechiae formation postoperatively, and ease of post-operative management (Biedlingmaier, 1993;Biedlingmaier, Whelan, Zoarski, and Rothman,

1996;Havas and Lowinger, 2000;Rice, 1998;Shih, Chin, and Rice, 2003;Stewart, 1998;Stammberger, 1986).

In contrast, surgeons who advocate preservation have argued that the MT is an essential surgical landmark, that its resection could contribute to a cerebrospinal fluid leak, anosmia, or frontal sinusitis, and disruption in nasal air conditioning, particle deposition, and airflow (Stammberger, 1986;Kennedy, 1998;Vleming, Middelweerd, and de, 1992). Nasal turbinates are believed to play a critical role in determining laminar airflow, efficient mixing of air for air conditioning, and nasal resistance (LaMear, Davis, Templer, McKinsey, and Del, 1992;Weinhold and Mlynski, 2004;Lindemann, Brambs, Keck, Wiesmiller, Rettinger, and Pless, 2005;Kelly, Prasad, and Wexler, 2000). Nasal obstruction often accompanies CRS, and the improvement of this symptom is crucial to a patient's perception of a successful therapeutic outcome (Damm, Quante, Jungehuelsing, and Stennert, 2002;Giger, Landis, Zheng, Malis, Ricchetti, Kurt, Morel, and Lacroix, 2003;Bhattacharyya, 2004a;Bhattacharyya, 2004b). Concerns about altering airflow and nasal resistance from middle turbinectomy has led some surgeons to preserve this structure, for fear of developing postoperative crusting and bleeding (Bhattacharyya, 2004a;LaMear, Davis, Templer, McKinsey, and Del, 1992;Cook, Begegni, Bryant, and Davis, 1995) or even paradoxical nasal obstruction. Although Cook et al. (Cook, Begegni, Bryant, and Davis, 1995) used rhinomanometry to demonstrate no deleterious effect on nasal airflow or resistance in a case series of 31 patients who underwent partial middle turbinectomy, recent modeling studies (Zhao, Scherer, Hajiloo, and Dalton, 2004) have shown that small alterations in nasal anatomy may alter local airflow and turbulence to a much greater extent than they alter total airflow. Given that standard methods of rhinometric assessment can only evaluate total airflow and resistance, a method is needed to evaluate the effects of MT resection on local airflow and shear stress perturbation in the complicated three-dimensional geometry of the nasal passages.

In this study, we applied CFD modeling of airflow in a patient's nose before and after surgery to determine the effect of partial MT resection on global and local nasal airflow.

Methods

Subject

A 68-year-old African American male presented with chronic left-sided nasal obstruction was identified for this study. The patient had a history of obstructive sleep apnea as well as mild left worse than right chronic rhinosinusitis that was poorly managed with medical therapy and aggravated by his Bilevel Positive Airway Pressure (BIPAP) treatment for apnea. CT scans showed bilateral mild mucosal thickening within patent osteomeatal units. The CT scans also revealed a large left middle concha bullosa, a contralateral septal deviation, and previously reduced inferior turbinates, all of which were confirmed by nasal endoscopy. As a retrospective study, no acoustic rhinometry or rhinomanometry studies were performed on this patient.

An endoscopic partial left middle turbinate resection with elimination of the concha bullosa was performed. Six weeks post-operatively, the patient continued to have some difficulty

with nasal congestion, facial pain and tolerance to BIPAP. Nasal endoscopy revealed scabbing at the surgical site and a mild fungal infection, which resolved within three months postoperatively, but without accompanying symptom resolution. CT scans acquired three months postoperatively demonstrated a partial left MT resection and mucosal thickening within the maxillary sinuses, which was somewhat worse when compared to pre-surgical imaging. The patient's complaints of left nasal obstruction persisted following surgery.

In the author's experience, few patients request surgery limited to the middle turbinate as a means of addressing a perceived ipsilateral nasal obstruction. This patient permitted us to explore the effects of partial middle turbinate resection without the variable of concurrent surgery on other portions of the nose. Additionally necessary for the present study, the pre-operative and three month post-operative coronal and axial CT scans of 1 mm thickness were available for CFD modeling.

Modeling procedure

Pre- and post-surgical three-dimensional numerical nasal models suitable for numerical simulation of nasal airflow were constructed for the patient based on his corresponding CT scans following the method described by Zhao *et al.* (Zhao, Scherer, Hajiloo, and Dalton, 2004;Zhao, Pribitkin, Cowart, Rosen, Scherer, and Dalton, 2006). The CT images of the patient were obtained from the medical imaging center at Thomas Jefferson University Hospital (Philadelphia, PA) using a Philips Mx view 8000 scanner (slice thickness =1 mm, field of view=20 cm, kVp=120, and mA=117) with a resolution of 512×512 pixel per image and a pixel size of 0.3906 mm^2.

To reconstruct each three-dimensional nasal model, first the interface between the nasal mucosa and the air was delineated (using AMIRA®) in the CT scans (see Figure 1). Then, the nasal cavity air space was filled with tetrahedral elements (ICEMCFD®). A finer mesh (prism layer) was created near the mucosal surface to more accurately resolve the rapidly changing near-wall air velocity profile (see Figure 1). Although mesh independence was not directly examined in this study, it was considered in previous work (Zhao, Scherer, Hajiloo, and Dalton, 2004). The current study followed the exact same meshing protocol of our previous study and the final mesh sizes are in the range of 1.7-1.9 million for pre- and post-surgery models, which were shown to be sufficient to accurately capture the flow phenomena of interest. Figure 2a shows the surfaces of the reconstructed pre-surgery nasal cavity model, displayed in different colors to distinguish the main nasal cavity from different sinuses.

Next, inspiratory and expiratory quasi-steady laminar nasal airflow (Keyhani, Scherer, and Mozell, 1997;Zhao, Scherer, Hajiloo, and Dalton, 2004;Zhao, Dalton, Yang, and Scherer, 2006) at resting breathing condition were simulated (Fluent©, Fluent Inc, USA) by applying a physiologically realistic pressure drop of 15 Pascal between the nostrils and the nasopharynx. The assumption of quasi-steady state laminar nasal airflow in the nasal cavity has been found to be appropriate for up to twice the resting breathing rate (Hahn, Scherer, and Mozell, 1993;Keyhani, Scherer, and Mozell, 1995). Nasal airflow becomes transitional or turbulent at higher flow rates, especially during sniffing. However, for most patients,

including this subject, their symptoms manifest at quiet breathing state. Thus, in this study, we limited our simulation to quiet restful breathing flow rate.

Several post processing analysis techniques allowed for the comparison of pre- and post-operative nasal airflow patterns and odorant delivery rates. Airflow rates were calculated by a surface integration of air velocity over the inlet and outlet planes (nostrils and nasopharynx). Contour plots of airflow velocity magnitude were generated on the same coronal cross sections on both pre- and post-surgery models. Airflow streamlines were generated by numerically releasing neutrally buoyant particles across the inlets (external naris for inhalation and nasopharynx for exhalation) and tracing the particle path. Wall surface shear stress and odorant (l-carvone) uptake flux to the mucosa in the olfactory cleft were also computed based on the airflow simulation results. l-carvone was chosen due to its high mucosa absorptive rate, the uptake flux of which was previously reported to be highly susceptible to local airflow changes (Kurtz, Zhao, Hornung, and Scherer, 2004;Zhao, Dalton, Yang, and Scherer, 2006). The boundary condition for odorant uptake at the air/

mucus interface is defined as: $\dfrac{\partial C'}{\partial y'} + KC' = 0$ (1) with $K = \dfrac{d_{in}D_m}{D_a\beta H_m}$, where C′ is the normalized l-carvone concentration, d_{in} is the hydraulic diameter (4×cross-sectional area / perimeter) of the nostril, D_m and D_a are the odorant diffusion coefficient in mucus and in air respectively, β is the air/mucus odorant partition coefficient (defined as the ratio of odorant concentration in air phase to the concentration in mucus at the air/mucus interface), H_m is the thickness of the mucus layer and also the length of the path through which odorant molecules diffuse. Further details and validation of these parameters can be found in (Kurtz, Zhao, Hornung, and Scherer, 2004).

Results

Table 1 shows the total inspiratory nasal flow rate (ml/s) through the left and right nostrils for the same pressure drop of 15 Pascal as predicted by pre- and post-surgical model simulations. The results indicate an increase (∼20%) in total nasal airflow or decrease in nasal resistance post-operatively and bilaterally. However, the reduction of nasal resistance on the non-operative (right) side approaches that on the operative (left) side suggesting that the reduction is due to a decrease in mucosal congestion rather than the partial MT resection. Neither acoustic rhinometry nor rhinomanometry were available in this retrospective study, but would be useful to corroborate these results. Regardless of the nasal resistance changes, however, the patient's symptom of left-sided nasal congestion persisted following surgery.

The patient's global nasal airflow pattern was within the normal range and did not change significantly on either side following surgery. However, the *local* airflow distribution did change significantly near the operative site (Figure 3), as shown in the pre- and post-operative contour plots of air velocity magnitude at six coronal sectional planes (Figure 2b). The match between the coronal cross section of our model and the CT images demonstrates the anatomical accuracy of the modeling technique. On the left (operative) side, a shift of the airflow distribution toward the removed concha bullosa area is observed post-operatively, with reduced airflow speeds. However, downstream from the surgery site, the airflow distribution appears to be similar to the pre-surgical state. This observation was

quantitatively confirmed by the plots of calculated fractional airflow flow rate (Figure 4a) and maximum airflow speed (m/s) (Figure 4b) in the nasal airway above the inferior turbinate (above the lower lines in Figure 3). In summary, MT resection resulted in a 38% increase in airflow rate and a 50% decrease in maximum airflow speed around the region of the concha bullosa. However, these values return to pre-surgical values either upstream or approximately 2.5 cm downstream away from the site. The increase in airway size and decrease in peak airflow speed also resulted in a corresponding decrease in shear stress on the mucosal wall near the surgery site, which was confirmed in the plot of maximum wall shear stress (Figure 4c). Local air pressure changes were also noticeable post-operatively (Figure 5) at the region of osteomeatal complex, despite a fixed overall pressure drop applied across the nasal cavity. Finally, no significant changes in the uptake flux of l-carvone (Figure 4d) onto the olfactory cleft mucosa (region above the upper lines in Figure 3) were observed post surgery.

CFD calculations on the non-operative side (right) for regional airflow rate, flow speed, wall shear stress and uptake flux show remarkable pre- and post operative consistency (Figure 4). Given the nasal dynamics (cycle) over time and the uncertainty introduced by the manual selection process of the region of interest, these results confirm the reproducibility and consistency of the modeling technique.

Discussion

Previous studies based on CFD modeling have shown that relatively small nasal anatomical changes can result in significant differences in nasal airflow patterns (Zhao, Scherer, Hajiloo, and Dalton, 2004;Zhao, Pribitkin, Cowart, Rosen, Scherer, and Dalton, 2006). Based on the study of this one patient, we observed that partial MT resection alone may not significantly affect overall nasal airflow patterns or flow distributions away from the operative site. Regionally, we did find that the increased airway volume after MT resection results in a shift in the regional airflow distribution towards this enlarged area, with decreased airflow speeds and wall shear stress and an increase in local air pressure. In this particular patient, the MT appears to be important in maintaining the regional airflow profile but not overall nasal airflow patterns and resistance. We suspect that this may be the reason why the patient's symptom of left-sided obstruction persisted post-surgery. Nevertheless, the importance of this alteration in the regional airflow profile of the osteomeatal complex in other functional aspects is subject to continuing debate. This alteration of airflow may disrupt local air-conditioning and mucosal water conservation.

Because the regional expansion of the nasal airway post-surgery could promote local transition of nasal airflow to turbulence, we computed the local Reynolds number for this particular patient in this region. With a Reynolds number of 554, turbulence was not a serious concern here, but should be further considered in future work. The reduced nasal airway wall shear stress at the surgical site may affect the regional mucociliary blanket dynamics and post-operative mucosal recovery, although this effect cannot be simulated by CFD. Finally, perturbation of the pressure gradient at the osteomeatal complex and frontal recess may impact the ventilation of the maxillary and frontal sinus. Swanson et al. (Swanson, Lanza, Kennedy, and Vining, 1995) have shown a statistically significant

increase in the incidence of frontal sinus disease after partial or total MT resection. The functional implication of local air pressure changes on air ventilation of the nasal sinuses, along with other airflow and air/mucosa interaction properties (shear stress, heat/water loss, etc.) awaits future investigations across a greater numbers of patients.

The impact of MT resection on olfaction has also been debated, and arguments for both improvement and impairment of olfactory function as a function of airflow changes have been proposed that include: 1) increased airway volume following MT resection could reduce nasal resistance and increase airflow and odorant transport to the olfactory cleft; or 2) MT resection could disrupt the patterns of normal airflow that channel odorant molecules to the olfactory cleft. In this patient, who reported no olfactory dysfunction pre- or post-operatively, partial MT resection had no significant effect on the uptake flux of l-carvone onto the olfactory cleft mucosa. L-carvone is highly sorptive in mucosa and its uptake appears to be highly susceptible to local airflow changes (Kurtz, Zhao, Hornung, and Scherer, 2004;Zhao, Dalton, Yang, and Scherer, 2006), making it an ideal candidate to probe the transport phase leading up to olfaction. Further supporting this statement, a recent clinical study successfully quantified the conductive factors associated with the olfactory losses in chronic rhinosinusitis patients based on their odor detection thresholds to l-carvone and the CFD simulations of individual l-carvone uptakes rates (Zhao, Jiang, Pribitkin, Dalton, Rosen, Lyman, Yee, Rawson, and Cowart, 2014). The decrease of l-carvone uptake flux over distance shown in this study in Figure 4d is due to the decrease of the remaining l-carvone concentration in the downstream airflow as the result of upstream mucosal absorption (Keyhani, Scherer, and Mozell, 1995) independent of individual differences, and evidently, the rates of decrease is similar between pre- vs post-surgery models and surgical vs. non-surgical sides in this case.

Biopsy studies (Feron, Perry, McGrath, and Mackay-Sim, 1998) that report sparse distribution of olfactory neurons on the septal anterior and middle portions of the MT, further complicate a thorough understanding of the impact of MT resection on olfaction. Both the loss of the olfactory mucosa surface following MT resection and the possible changes in local airflow rates and odorant uptake flux warrant further investigation across larger patient populations. Detailed CFD analyses of these outcomes may contribute to the understanding of the functional impact of MT surgery on olfaction.

In general, no quantitative method has been able to satisfactorily predict how or if the removal of tissue during FESS will impact nasal obstruction or other nasal functions (including olfaction). Neither CT nor outcome studies using standard rhinometric assays (e.g. acoustic rhinometry and rhinomanometry) indexing global airflow changes have proven conclusive. Indeed, decreased global or regional nasal resistance may not correlate with clinical outcomes. In the future, quantitative modeling studies across larger and more varied patient populations may reveal a link between subjective symptoms and properties such as airflow patterns, pressure, shear stress, etc. Such attempt has recently been performed on a cohort of healthy subjects (n=22) (Zhao and Jiang, 2014). Future goals should include using CFD modeling as described here to prospectively determine surgical strategies to optimize local airflow profiles based on the results of the normative studies. Such a prospective and quantitative evaluation of surgical outcomes may serve as an

important pre-operative guide in determining the extent and technique of surgery. Conceivably, a CFD based pre-surgical simulation could be converted to a CT scan format and loaded into an image guidance system for use during surgery. An image guidance system offers the surgeon a real-time tracking of where the endoscope probe or the cutting tips are located inside the nasal sinus during the surgery in three orthogonal CT image slices displayed on a computer screen. The surgeon could remove tissue until real time images matched the landmarks delineated in the CFD model.

Conclusion

We have demonstrated the feasibility and the advantages of CFD nasal airflow modeling in a patient with a unilateral concha bullosa who underwent partial MT resection. In this particular patient, partial MT resection did not impact overall nasal airflow patterns and resistance, but did alter the regional airflow profile proximal to the osteomeatal complex.

The ability to predict the effect of middle turbinectomy on nasal airflow patterns may prove valuable in future clinical studies. Although we focused on airflow velocity, streamlines, shear stress, and pressure drop in this study, the CFD technique could be used to investigate other airflow properties, such as water vapor exchange (for drying), heat loss (Zhao, Jiang, Blacker, Lyman, Dalton, Cowart, and Pribitkin, 2013;Zhao, Dalton, Cowart, and Pribitkin, 2014), etc., which may lead to a fuller understanding of the impact of MT resection on nasal physiology and symptoms.

In the future, such modeling techniques may be widely applied to other nasal sinus surgical procedures and could be used as a personalized, patient-specific pre-surgical planning tool to guide the optimization of airflow and odorant delivery in the human nose.

Acknowledgments

Literature Cited

Bhattacharyya N. Clinical outcomes after revision endoscopic sinus surgery. Arch Otolaryngol Head Neck Surg. 2004a; 130:975–978. [PubMed: 15313869]

Bhattacharyya N. Symptom outcomes after endoscopic sinus surgery for chronic rhinosinusitis. Arch Otolaryngol Head Neck Surg. 2004b; 130:329–333. [PubMed: 15023842]

Biedlingmaier JF. Endoscopic sinus surgery with middle turbinate resection: results and complications. Ear Nose Throat J. 1993; 72:351–355. [PubMed: 8334966]

Biedlingmaier JF, Whelan P, Zoarski G, Rothman M. Histopathology and CT analysis of partially resected middle turbinates. Laryngoscope. 1996; 106:102–104. [PubMed: 8544615]

Cook PR, Begegni A, Bryant WC, Davis WE. Effect of partial middle turbinectomy on nasal airflow and resistance. Otolaryngol Head Neck Surg. 1995; 113:413–419. [PubMed: 7567014]

Damm M, Quante G, Jungehuelsing M, Stennert E. Impact of functional endoscopic sinus surgery on symptoms and quality of life in chronic rhinosinusitis. Laryngoscope. 2002; 112:310–315. [PubMed: 11889389]

Feron F, Perry C, McGrath JJ, Mackay-Sim A. New techniques for biopsy and culture of human olfactory epithelial neurons. Archives of Otolaryngology,Head and Neck Surgery. 1998; 124:861–866. [PubMed: 9708710]

Garcia GJ, Rhee JS, Senior BA, Kimbell JS. Septal deviation and nasal resistance: an investigation using virtual surgery and computational fluid dynamics. Am J Rhinol Allergy. 2010; 24:e46–e53. [PubMed: 20109325]

Giger R, Landis BN, Zheng C, Malis DD, Ricchetti A, Kurt AM, Morel DR, Lacroix JS. Objective and subjective evaluation of endoscopic nasal surgery outcomes. Am J Rhinol. 2003; 17:327–333. [PubMed: 14750607]

Girardin M, Bilgen E, Arbour P. Experimental study of velocity fields in a human nasal fossa by laser anemometry. Ann Otol Rhinol Laryngol. 1983; 92:231–236. [PubMed: 6222682]

Grant O, Bailie N, Watterson J, Cole J, Gallagher G, Hanna B. Numerical model of a nasal septal perforation. Medinfo. 2004; 11:1352–1356.

Hahn I, Scherer PW, Mozell MM. Velocity profiles measured for airflow through a large-scale model of the human nasal cavity. J Appl Physiol. 1993; 75:2273–2287. [PubMed: 8307887]

Havas TE, Lowinger DS. Comparison of functional endonasal sinus surgery with and without partial middle turbinate resection. Ann Otol Rhinol Laryngol. 2000; 109:634–640. [PubMed: 10903043]

Ho WK, Yuen AP, Tang KC, Wei WI, Lam PK. Time course in the relief of nasal blockage after septal and turbinate surgery: a prospective study. Arch Otolaryngol Head Neck Surg. 2004; 130:324–328. [PubMed: 15023841]

Hornung DE, Leopold DA, Youngentob SL, Sheehe PR, Gagne GM, Thomas FD, Mozell MM. Airflow patterns in a human nasal model. Arch Otolaryngol Head Neck Surg. 1987; 113:169–172. [PubMed: 3801173]

Kelly JT, Prasad AK, Wexler AS. Detailed flow patterns in the nasal cavity. J Appl Physiol. 2000; 89:323–337. [PubMed: 10904068]

Kennedy D. Middle turbinate resection: evaluating the issues: should we resect normal middle turbinates? Arch Otolaryngol Head Neck Surg. 1998; 124:107–112. [PubMed: 9440792]

Keyhani K, Scherer PW, Mozell MM. Numerical simulation of airflow in the human nasal cavity. J Biomech Eng. 1995; 117:429–441. [PubMed: 8748525]

Keyhani K, Scherer PW, Mozell MM. A numerical model of nasal odorant transport for the analysis of human olfaction. J Theor Biol. 1997; 186:279–301. [PubMed: 9219668]

Kurtz DB, Zhao K, Hornung DE, Scherer PW. Experimental and numerical determination of odorant solubility in nasal and olfactory mucosa. Chem Senses. 2004; 29:763–773. [PubMed: 15574812]

LaMear WR, Davis WE, Templer JW, McKinsey JP, Del PH. Partial endoscopic middle turbinectomy augmenting functional endoscopic sinus surgery. Otolaryngol Head Neck Surg. 1992; 107:382–389. [PubMed: 1408223]

Lindemann J, Brambs HJ, Keck T, Wiesmiller KM, Rettinger G, Pless D. Numerical simulation of intranasal airflow after radical sinus surgery. Am J Otolaryngol. 2005; 26:175–180. [PubMed: 15858773]

Martonen TB, Quan L, Zhang Z, Musante CJ. Flow simulation in the human upper respiratory tract. Cell Biochem Biophys. 2002; 37:27–36. [PubMed: 12398415]

Ozlugedik S, Nakiboglu G, Sert C, Elhan A, Tonuk E, Akyar S, Tekdemir I. Numerical study of the aerodynamic effects of septoplasty and partial lateral turbinectomy. Laryngoscope. 2008; 118:330–334. [PubMed: 18030167]

Proetz AW. Air currents in the upper respiratory tract and their clinical importance. Ann Octol Rhinol Laryngol. 1951; 60:439–467.

Rice DH. Middle turbinate resection: weighing the decision. Arch Otolaryngol Head Neck Surg. 1998; 124:106. [PubMed: 9440791]

Shih C, Chin G, Rice DH. Middle turbinate resection: impact on outcomes in endoscopic sinus surgery. Ear Nose Throat J. 2003; 82:796–797. [PubMed: 14606177]

Stammberger H. Endoscopic endonasal surgery--concepts in treatment of recurring rhinosinusitis. Part II. Surgical technique. Otolaryngol Head Neck Surg. 1986; 94:147–156. [PubMed: 3083327]

Stewart MG. Middle turbinate resection. Arch Otolaryngol Head Neck Surg. 1998; 124:104–106. [PubMed: 9440790]

Stewart MG, Smith TL, Weaver EM, Witsell DL, Yueh B, Hannley MT, Johnson JT. Outcomes after nasal septoplasty: results from the Nasal Obstruction Septoplasty Effectiveness (NOSE) study. Otolaryngol Head Neck Surg. 2004; 130:283–290. [PubMed: 15054368]

Subramaniam RP, Richardson RB, Morgan KT, Kimbell JS. Computational fluid dynamics simulations of inspiratory airflow in the human nose and nasopharynx. Inhal Toxicol. 1999; 10:91–120.

Swanson P, Lanza DC, Kennedy DW, Vining EM. The effect of middle turbinate resection upon frontal sinus disease. Am J Rhinol. 1995; 9:191–195.

swift, DL.; Proctor, DF. Access of air to the respiratory tract. In: Brain, JD.; Proctor, DF.; Reid, LM., editors. Respiratory defense mechanism. New York: Marcel Dekker Inc.; 1977. p. 63-91.

Vleming M, Middelweerd RJ, de VN. Complications of endoscopic sinus surgery. Arch Otolaryngol Head Neck Surg. 1992; 118:617–623. [PubMed: 1637539]

Weinhold I, Mlynski G. Numerical simulation of airflow in the human nose. Eur Arch Otorhinolaryngol. 2004; 261:452–455. [PubMed: 14652769]

Wexler D, Segal R, Kimbell J. Aerodynamic effects of inferior turbinate reduction: computational fluid dynamics simulation. Arch Otolaryngol Head Neck Surg. 2005; 131:1102–1107. [PubMed: 16365225]

Wolf JS, Biedlingmaier JF. The middle turbinate in endoscopic sinus surgery. Current opinion in Otolaryngology & Head & Neck Surgery. 2001; 9:23–26.

Zhao K, Dalton P, Cowart BJ, Pribitkin EA. Re: In response to Regional Peak Mucosal Cooling Predicts the Perception of Nasal Patency. Laryngoscope. 2014 May; 124(5):E211–2.10.1002/lary. 24621 [PubMed: 24474709]

Zhao K, Dalton P, Yang GC, Scherer PW. Numerical Modeling of Turbulent and Laminar Airflow and Odorant Transport during Sniffing in the Human and Rat Nose. Chem Senses. 2006; 31:107–118. [PubMed: 16354744]

Zhao K, Jiang J. What is normal nasal airflow? A computational study of 22 healthy adults. Int Forum Allergy Rhinol. 2014 Jun; 4(6):435–46.10.1002/alr.21319 [PubMed: 24664528]

Zhao K, Jiang J, Blacker K, Lyman B, Dalton P, Cowart BJ, Pribitkin EA. Regional peak mucosal cooling predicts the perception of nasal patency. Laryngoscope. 2014 Mar; 124(3):589–95. Epub. 10.1002/lary.24265 [PubMed: 23775640]

Zhao K, Jiang J, Pribitkin EA, Dalton P, Rosen D, Lyman B, Yee KK, Rawson NE, Cowart BJ. Conductive olfactory losses in chronic rhinosinusitis? A computational fluid dynamics study of 29 patients. Int Forum Allergy Rhinol. 2014 Apr; 4(4):298–308. Epub. 10.1002/alr.21272 [PubMed: 24449655]

Zhao K, Pribitkin EA, Cowart BJ, Rosen D, Scherer PW, Dalton P. Numerical modeling of nasal obstruction and endoscopic surgical intervention: outcome to airflow and olfaction. American Journal of Rhinology. 2006; 20:308–316. [PubMed: 16871935]

Zhao K, Scherer PW, Hajiloo SA, Dalton P. Effect of anatomy on human nasal air flow and odorant transport patterns: implications for olfaction. Chem Senses. 2004; 29:365–379. [PubMed: 15201204]
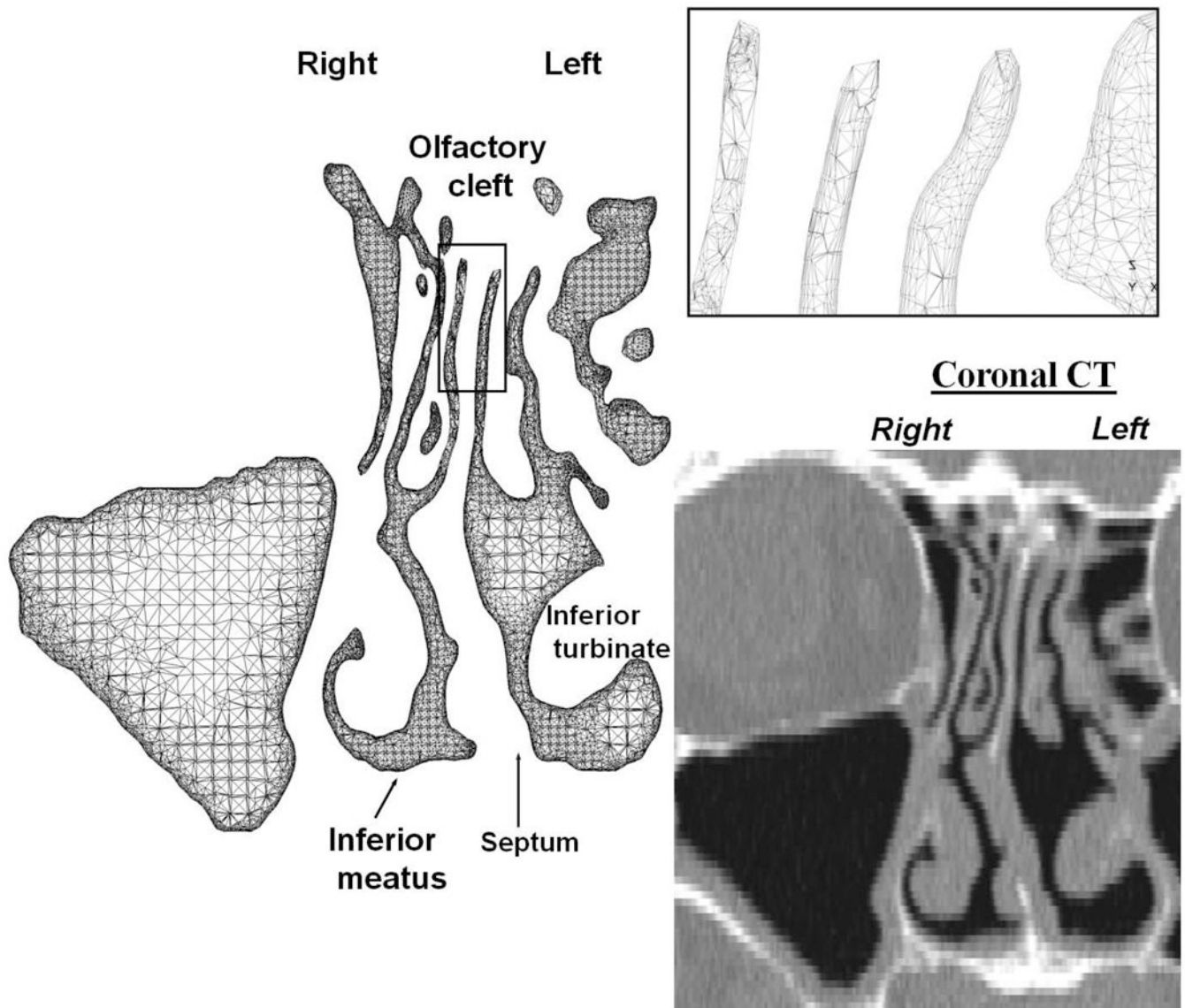
Figure 1.
Coronal cross section of a nasal CFD model and the corresponding CT image. The whole nasal model consists of 1.7 million tetrahedral elements, with layers of small and fine elements along the wall (see the inset) in order to resolve the near wall changes of air velocity and odorant concentration profile.
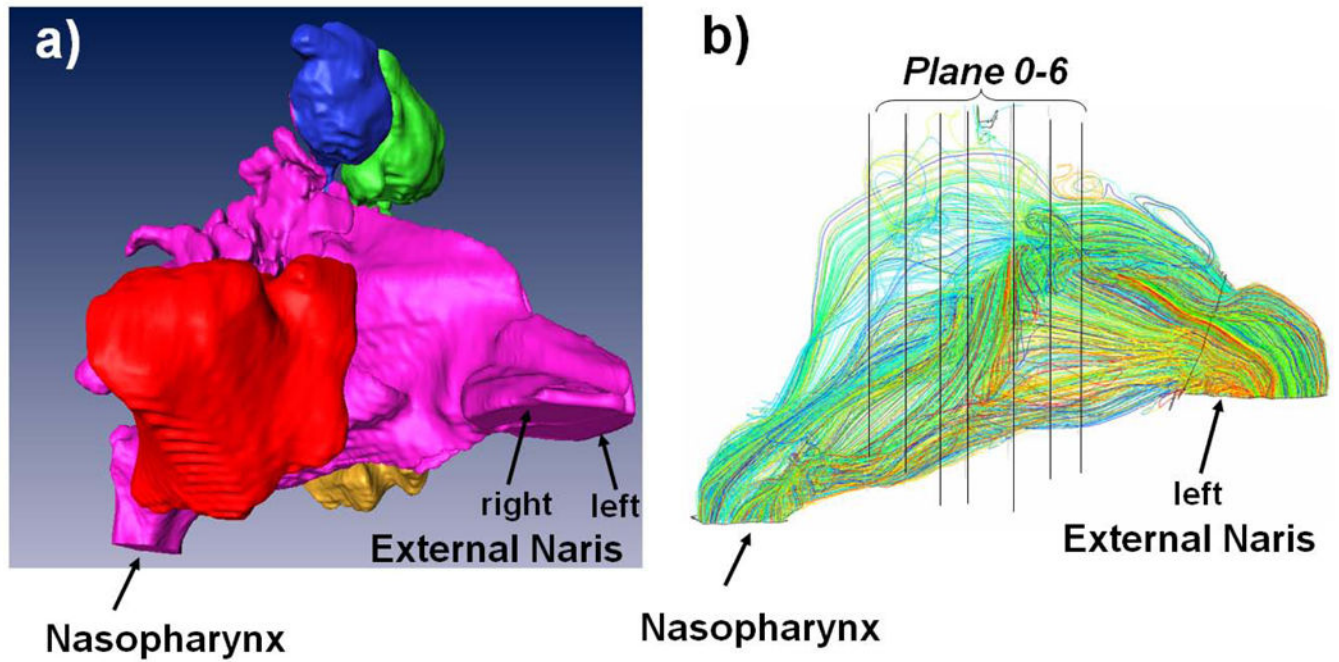
Figure 2.
a) Nasal CFD models of one patient who underwent partial middle turbinate resection surgery. Only the pre-surgery model is shown, with airway wall displayed in different colors to distinguish the main nasal cavity from different sinuses. **b)** Airflow streamlines in the left side post-surgery nasal model. In general, the patterns do not differ significantly with pre-surgery model (not shown).
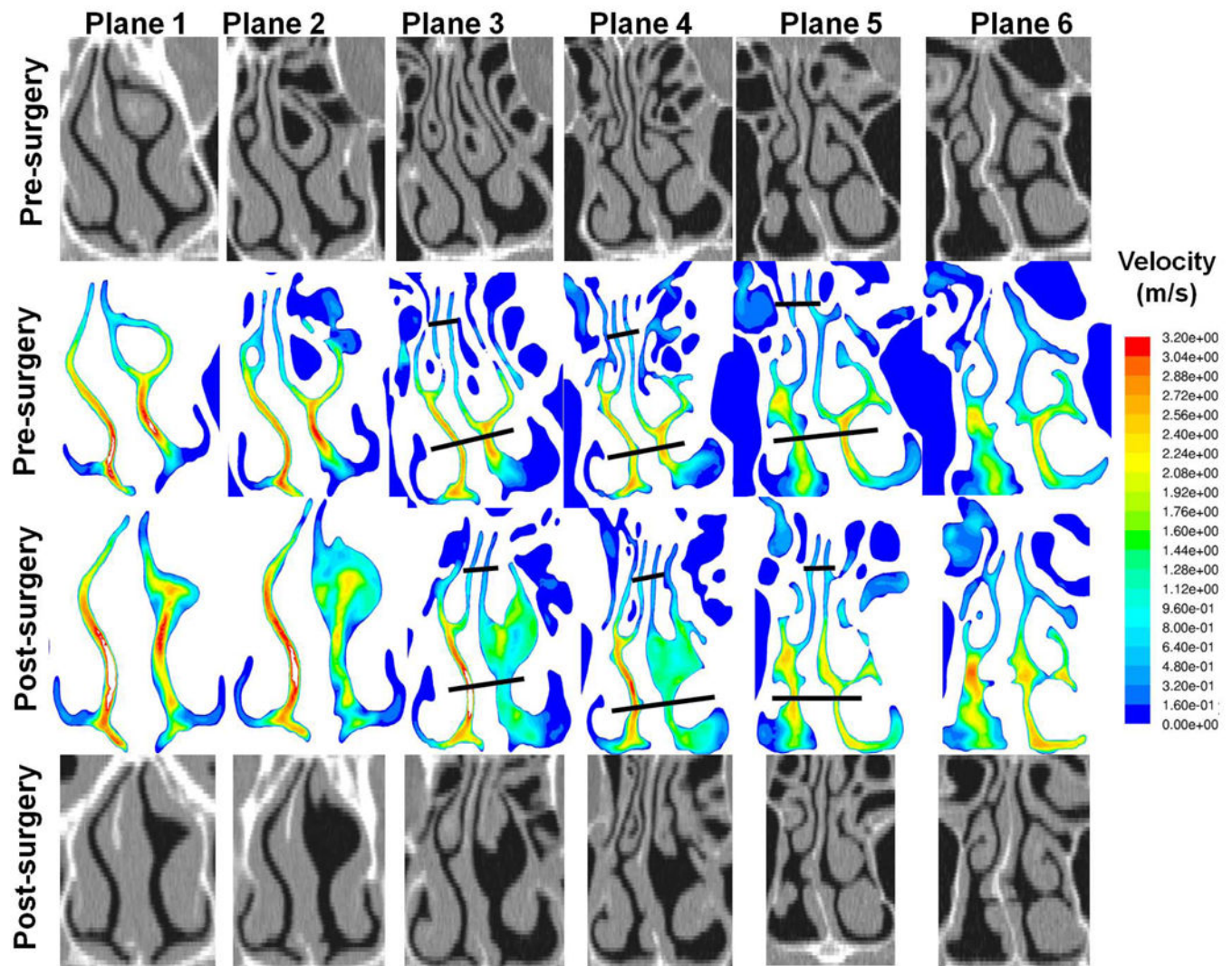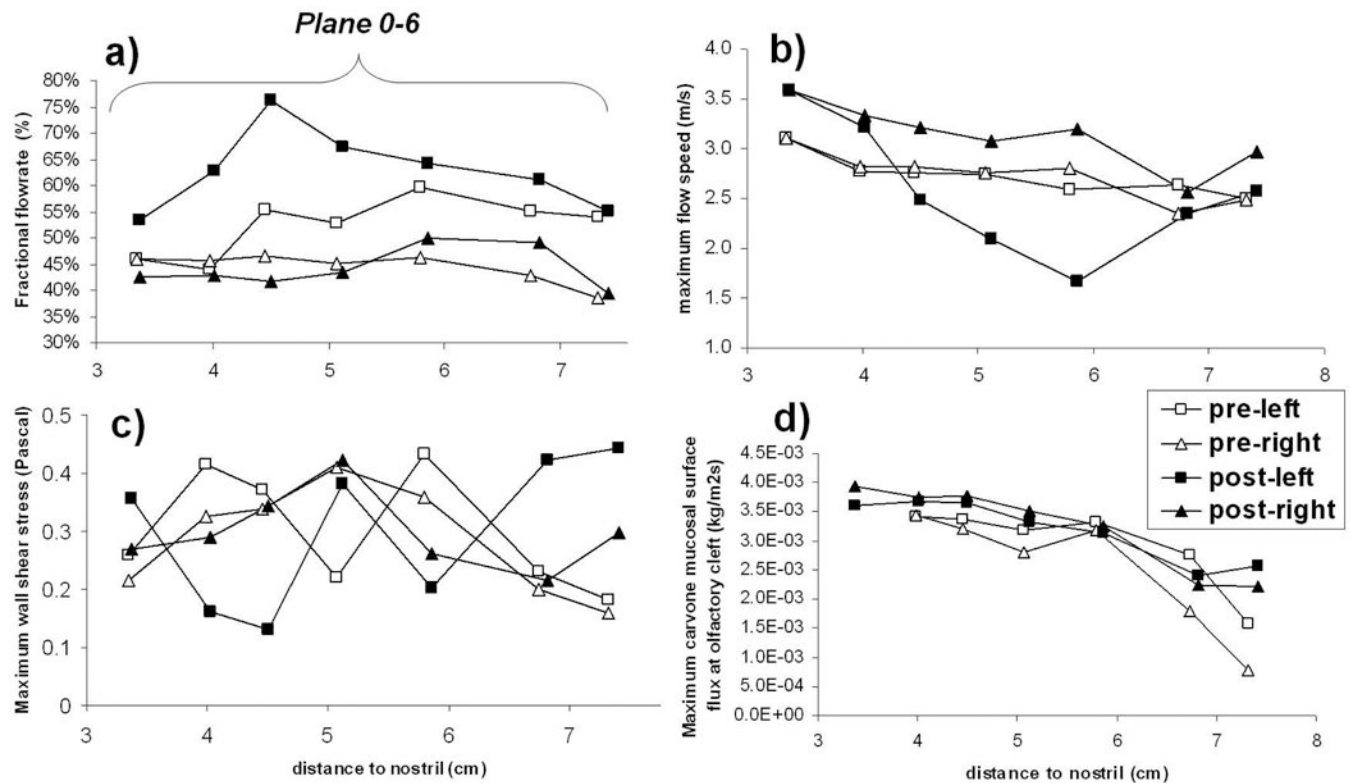
Figure 3.

Contour plot of pre- (2nd row) and post- (3rd row) surgery inspiratory velocity magnitude for a pressure drop of 15 Pascal on 7 coronal planes (as indicated in Figure 2b), along with the pre- (1st row) and post-surgery (4th row) coronal CT scans. The close match between the coronal cross section of the post-surgical model and the CT images demonstrates the anatomical accuracy of our modeling technique. The lower lines define the "airway above inferior turbinate" for calculation in Figure 4. The airway above the upper lines roughly represents the "olfactory cleft" (0.7 cm from the superior tip of the cleft) for calculation in Figure 4d.

Figure 4.
Calculated **a)** fractional airflow rate (ratio of local airflow rate to the total airflow rate in ml/s through each nostril) **b)** maximum airflow speed (m/s) **c)** maximum nasal airway wall shear stress (Pascal) in or through the nasal airway above the inferior turbinate (above the lower lines in Figure 3) at the 7 coronal planes (0-6, in Figure 2b) in the right (non-operative, $\triangle\blacktriangle$ triangle) and left (operative, $\square\blacksquare$ square) side and pre- ($\triangle\square$ empty) and post-surgery ($\blacktriangle\blacksquare$ solid). In summary, these data indicate an increase in fractional airflow rate (by 38%), a decrease in maximum airflow speed (by 50%), and a corresponding decrease in wall shear stress (by 65%) around the region of the concha bullosa site post-surgery. However, the values return to pre-surgery values both upstream and downstream from the site. **d)** Calculated maximum odorant (l-carvone) uptake flux (Kg/m^2s) onto the nasal mucosa in the olfactory cleft (above the upper lines in Figure 3) at the 7 coronal planes (0-6, in Figure 2b) in the right (non-operative) and left (operative) side pre- and post-surgery. These results show that middle turbinate resection has no significant effect on the olfactory uptake flux. The decrease of uptake flux with distance is due to the decrease of the remaining l-carvone concentration in the downstream airflow as a result of the upstream mucosa absorption. Results on the non-operative side (right) show remarkable consistency between the pre- and post-operative models.
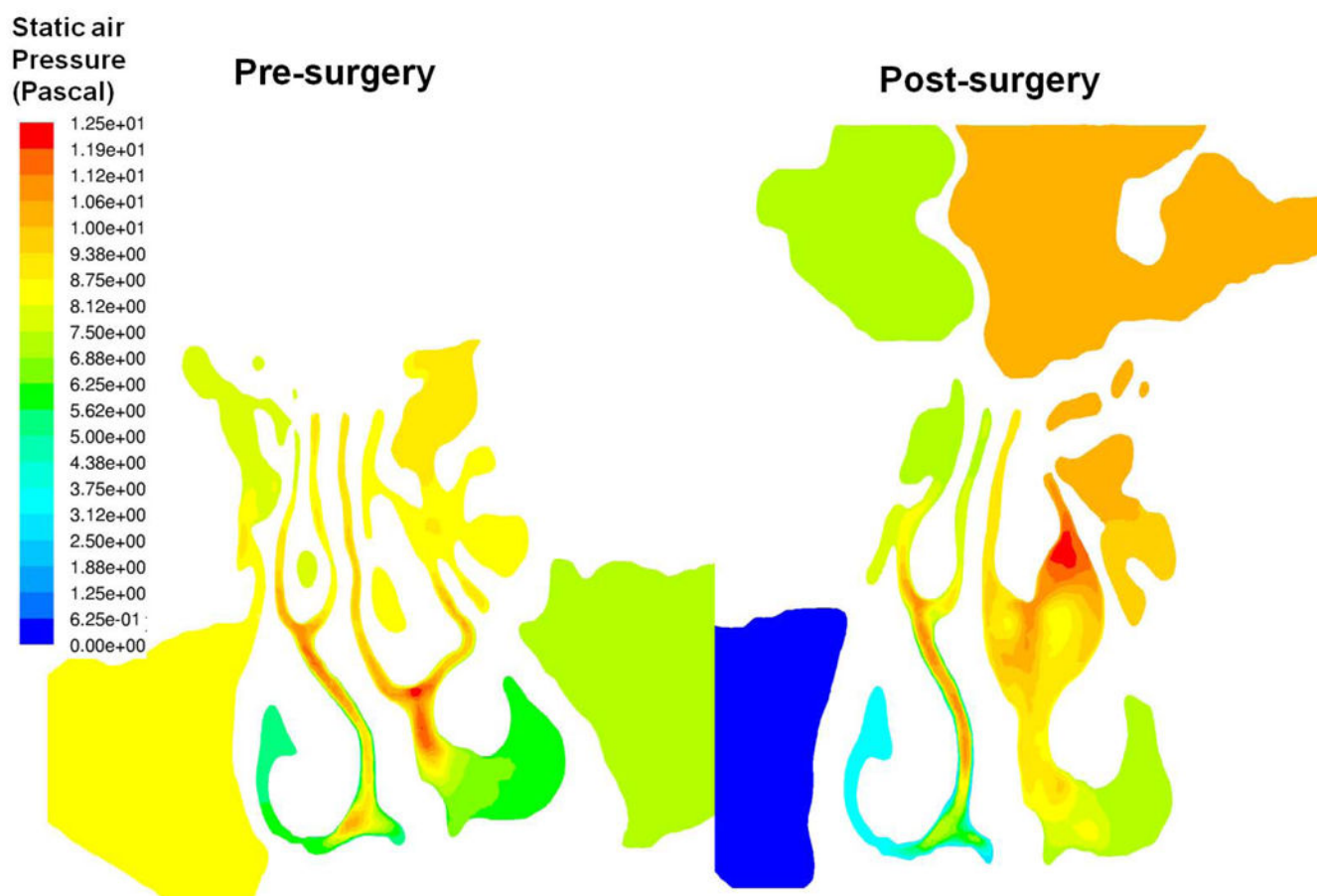
Figure 5.
Contour plot of pre- and post-surgery static air pressure (Pascal) on coronal plane 4 in Figure 3.

Table 1

Total nasal flow rate (ml/s) through the left and right nostrils for the same pressure drop of 15 Pascal across the nasal cavity predicted in pre- and post-surgical simulations.

	Pre- surgery	Post-surgery
Left (operation side)	160.2	191.1
Right (non-operation side)	156.1	189.4